Mechanics of Materials 81 (2015) 56–61

Contents lists available at ScienceDirect

Mechanics of Materials

journal homepage: www.elsevier.com/locate/mechmat

Transient analysis of multiple parallel cracks under anti-plane dynamic loading

K.-C. Wu *, Y.-L. Hou, S.-M. Huang

Institute of Applied Mechanics, National Taiwan University, Taipei, Taiwan

ARTICLE INFO

Article history:
Received 16 January 2014
Received in revised form 21 October 2014
Available online 30 October 2014

Keywords:
Non-collinear cracks
Dynamic stress intensity factor
Dislocation method

ABSTRACT

The problem of a homogeneous linear elastic body containing multiple non-collinear cracks under anti-plane dynamic loading is considered in this work. The cracks are simulated by distributions of dislocations and an integral equation relating tractions on the crack planes and the dislocation densities is derived. The integral equation in the Laplace transform domain is solved by the Gaussian–Chebyshev integration quadrature. The dynamic stress intensity factor associated with each crack tip is calculated by a numerical inverse Laplace scheme. Numerical results are given for one crack and two or three parallel cracks under normal incidence of a plane horizontally shear stress wave.

1. Introduction

One of the popular methods for solving crack problems with static loading is the dislocation method. In this method the tractions arising along the lines of the cracks in an uncracked body are determined first. The cracks are then inserted and the unsatisfied tractions canceled by inserting continuously varying density of dislocations, along the lines of the cracks. This formulation leads to an integral equation which may be discretized using Gaussian–Chebyshev quadrature to the desired degree of refinement (Erdogan et al., 1973). Once the resulting simultaneous linear equations are solved the stress intensity factors can be readily determined from the dislocation densities at the crack tips. The dislocation method, however, has rarely been applied to the problems concerning dynamic loading.

Cochard and Madariaga (1994) have essentially extended the dislocation method for a crack under dynamic anti-plane shear (mode III) loading. A space–time convolution integral equation was derived, which is Cauchy-singular in space as in the static case. In addition, there is another term associated with radiation damping by wave emission. Morrissey and Geubelle (1997) discussed the numerical implementation of a spectral scheme, in which the Fourier transform with respect to space was applied to the integral equation and the resulting equation in time was solved. Chen and Tang (1996) obtained an integral equation similar to that in Cochard and Madariaga (1994) but did not include the radiation damping term. Nevertheless they showed that if the Laplace transform in time was applied to the integral, the Cauchy singularity was preserved and the same integration quadrature for static loading might be employed. Wu and Chen (2011) have applied the integral equation of Cochard and Madariaga (1994) to treat the problem of multiple collinear cracks subjected to normal incidence of horizontally shear (SH) wave. Wu et al. (2013) have derived a similar integral equation for collinear cracks loaded by dynamic tensile loading.

The afore-mentioned works are for collinear cracks. There are very few papers on non-collinear cracks. Takakuda et al. (1984) used the integral transform method to solve the problem of two completely overlapping parallel cracks under normal incidence of SH wave. Ayatollahi

* Corresponding author. Tel.: +886 02 33665695; fax: +886 02 33665696.
E-mail address: wukciam@ntu.edu.tw (K.-C. Wu).

http://dx.doi.org/10.1016/j.mechmat.2014.10.006
0167-6636/

and Monfared (2012) have applied the dislocation technique to treat arbitrary multiple cracks. However, as in the case of Chen and Tang (1996), the radiation damping term was missing in the integral equation they derived. In this paper, an integral equation for non-collinear parallel cracks is properly derived based on the fundamental dynamic solution of a screw dislocation. The integral equation is then applied to solve the problem of two or three parallel cracks to demonstrate the accuracy and effectiveness of the dislocation method.

2. Basic equations

The equation of motion in anti-plane shear deformation is

$$\sigma_{31,1} + \sigma_{32,2} = \rho \frac{\partial^2 u}{\partial t^2}, \tag{1}$$

where u is the displacement in the x_3 direction, ρ is the mass density, t is time, and a comma in the subscript denotes partial differentiation. The stress–strain relations for isotropic materials are

$$\sigma_{3\alpha} = \mu u_{,\alpha}, \quad \alpha = 1, 2, \tag{2}$$

where μ is the shear modulus. The equation of motion in terms of the displacement is given by substituting Eq. (2) into Eq. (1) as

$$u_{,11} + u_{,22} = \frac{1}{c^2}\frac{\partial^2 u}{\partial t^2}, \tag{3}$$

where $c = \sqrt{\mu/\rho}$ is the shear wave speed.

If $u = u(y_1, y_2)$, where $y_1 = x_1/t$ and $y_2 = x_2/t$, the general solution of Eq. (3) may be represented as (Wu, 1999)

$$u = 2\mathrm{Re}[f(w)], \tag{4}$$

where Re stands for the real part and w is defined by

$$w = y_1 + p(w) y_2. \tag{5}$$

The function $p(w)$ is determined by substituting Eq. (4) into Eq. (3) as

$$p(w) = \sqrt{(w/c)^2 - 1}. \tag{6}$$

From Eqs. (5) and (6), w is given by

$$w = \frac{y_1 + y_2\sqrt{(y/c)^2 - 1}}{1 - (y_2/c)^2}, \tag{7}$$

where $y = \sqrt{y_1^2 + y_2^2}$. Eq. (4) is valid for $y < c$. For $y > c$, Eq. (4) can be continued along the constant w-line, which is tangent to the bulk shear wavefront $y = c$. From Eq. (2) σ_{32} can be expressed as

$$\sigma_{32} = 2\mu\mathrm{Re}\left[f'(w)\frac{\partial w}{\partial x_2}\right], \tag{8}$$

where $f'(w)$ denotes the derivative of f with respect to w.

3. Fundamental solution

Consider an infinite body that is stress-free and at rest everywhere at $t = 0$. A screw dislocation of the Burgers vector β appears at the origin for $t > 0$. The slip plane is assumed to coincide with the negative x_1-axis. The corresponding jump condition for u and continuity condition for σ_{32} at $x_2 = 0$ are given by

$$u^+(x_1, t) - u^-(x_1, t) = \beta H(t) H(-x_1), \tag{9}$$

$$\sigma_{32}(x_1, t)^+ - \sigma_{32}(x_1, t)^- = 0, \tag{10}$$

where the superscript $\pm$ denotes the limit as $x_2 \to 0^{\pm}$ and H is the Heaviside step function. Substitution of Eqs. (4) and (8) into Eqs. (9) and (10), respectively, for $t > 0$ yields

$$(f^+ - f^-) + (\bar{f}^- - \bar{f}^+) = \beta H(-x_1), \tag{11}$$

$$(f'^+ - f'^-) - (\bar{f}'^- - \bar{f}'^+) = 0, \tag{12}$$

The solution of $f(w)$ is obtained as

$$f(w) = \frac{\beta}{4\pi i}\ln w. \tag{13}$$

Substitution of Eq. (13) into Eqs. (4) and (8) gives

$$u = \frac{\beta}{2\pi}\mathrm{Im}(\ln w). \tag{14}$$

Substituting Eq. (7) into Eq. (14) yields

$$u = \frac{\beta}{2\pi}\tan^{-1}\left(\sqrt{1 - (y/c)^2}\tan\theta\right)H(c - y), \tag{15}$$

for $y < c$, where $\tan\theta = x_2/x_1$. Note that as $y \to 0$, which is corresponding to $r \to 0$ or $t \to \infty$, Eq. (15) recovers the well-known static solution:

$$u = \frac{\theta\beta}{2\pi}. \tag{16}$$

From Eq. (15) the displacement as $y \to c$ is

$$\begin{aligned} u &= \beta/2, \quad \pi/2 < \theta < \pi \\ &= 0, \quad -\pi/2 < \theta < \pi/2 \\ &= -\beta/2, \quad -\pi < \theta < -\pi/2 \end{aligned} \tag{17}$$

Thus continuation of the displacement for $y > c$ along the line tangent to the wavefront $y = c$ leads to

$$u = \frac{\beta}{2}[2H(y_2) - H(y_2 + c) - H(y_2 - c)]H(-y_1). \tag{18}$$

The wavefronts generated by the dislocation are shown in Fig. 1. From Eqs. (15) and (18), σ_{32} is given as

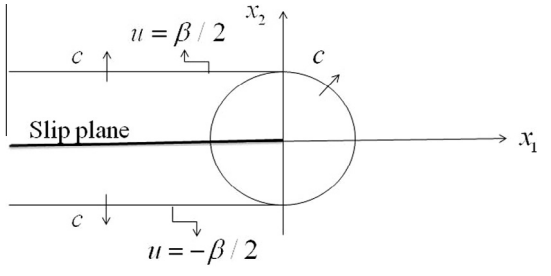

Fig. 1. The wavefronts generated by a dislocation of Burgers vector β that suddenly appears in an infinite body with shear wave speed c.

$$\sigma_{32} = -\frac{\mu\beta}{2c}H(-x_1)\delta(t-|x_2|/c) + \frac{\mu\beta}{2\pi}\frac{\cos\theta}{r}T(r,\theta,t), \tag{19}$$

where $r = \sqrt{x_1^2 + x_1^2}$ and

$$T(r,\theta,t) = \frac{t(t^2 - \left(\frac{r}{c}\right)^2 - \left(\frac{r\sin\theta}{c}\right)^2)}{\sqrt{t^2 - \left(\frac{r}{c}\right)^2}\left[t^2 - \left(\frac{r\sin\theta}{c}\right)^2\right]}H(t-r/c). \tag{20}$$

The first term on the right side of Eq. (19) is associated with the plane wave emitted from the slip plane and the second term the bulk wave radiated from the dislocation core as shown in Fig. 1. The result obtained by Ayatollahi and Monfared (2012) contains only the second term of Eq. (19).

4. Integral equation for multiple parallel cracks

Consider first a crack located at $|x_1 - b| \leqslant a$ and $x_2 = h$ in an infinite body subjected to an applied dynamic loading $\sigma_{32} = \sigma_0(x_1, x_2, t)$. It is assumed that the crack is loaded only for $t > 0$. By simulating the crack as a continuous distribution of dislocations, the relative crack face displacement, regarded as the Burgers vector β, may be represented as

$$\beta(x_1,h,t) = H(t)\int_{x_1}^{b+a}\int_0^t \dot{\alpha}(\xi_1,h,\tau)d\tau d\xi_1, \tag{21}$$

where $\dot{\alpha}$ is the time rate of the dislocation density. The crack closure condition requires

$$\beta(b-a,h,t) = H(t)\int_{b-a}^{b+a}\int_0^t \dot{\alpha}(\xi_1,h,\tau)d\tau d\xi_1 = 0. \tag{22}$$

From Eq. (19) and the principle of superposition, the total stress σ_{32} due to the dislocations and the applied loading for $t > 0$ is

$$\begin{aligned}\sigma_{32}(x_1,x_2,t) = &-\frac{\mu}{2c}\int_{x_1}^{b+a}\dot{\alpha}\left(\xi_1,h,t-\frac{|x_2-h|}{c}\right)d\xi_1 H\left(t-\frac{|x_2-h|}{c}\right)\\ &\times H(a-|x_1-b|) + \frac{\mu}{2\pi}\int_{b-a}^{b+a}\frac{\cos\theta'}{r'}\int_0^t T(r',\theta',t')\dot{\alpha}(\xi_1,h,\tau)d\tau d\xi_1\\ &+\sigma_0(x_1,x_2,t),\end{aligned} \tag{23}$$

where $r' = \sqrt{(x_1-\xi_1)^2 + (x_2-h)^2}$, $\theta' = \tan^{-1}\frac{x_2-h}{x_1-\xi_1}$ and $t' = t-\tau$. At $x_2 = h$, Eq. (23) becomes

$$\begin{aligned}\sigma_{32}(x_1,h,t) = &-\frac{\mu}{2c}\int_{x_1}^{b+a}\dot{\alpha}(\xi_1,h,t)d\xi_1 H(a-|x_1-b|)\\ &+\frac{\mu}{2\pi}\int_{b-a}^{b+a}\int_0^t \frac{\sqrt{1-\left(\frac{x_1-\xi_1}{c(t-\tau)}\right)^2}}{x_1-\xi_1}\dot{\alpha}(\xi_1,h,\tau)d\tau d\xi_1\\ &+\sigma_0(x_1,h,t).\end{aligned} \tag{24}$$

Eq. (24) is the same as that derived by Cochard and Madariaga (1994).

Taking the Laplace transform in time of Eq. (23) yields

$$\begin{aligned}\hat{\sigma}_{32}(x_1,x_2,s) = &-\frac{\mu s}{2c}e^{\frac{-|x_2-h|}{c}s}\int_{x_1}^{b+a}\hat{\alpha}(\xi_1,h,s)d\xi_1 H(a-|x_1-b|)\\ &+\frac{\mu s}{2\pi}\int_{b-a}^{b+a}\frac{\hat{T}(r',\theta',s)}{x_1-\xi_1}\hat{\alpha}(\xi_1,h,s)d\xi_1 + \hat{\sigma}_0(x_1,x_2,s),\end{aligned} \tag{25}$$

where a hat over a function is used to indicate the Laplace transform of the function. At the crack line, $|x_1 - b| \leqslant a$ and $x_2 = h$, $\sigma_{32} = 0$ and Eq. (25) gives

$$\begin{aligned}\hat{\sigma}_0(x_1,h,s) = &\frac{\mu s}{2c}\int_{x_1}^{b+a}\hat{\alpha}(\xi_1,h,s)d\xi_1\\ &+\frac{\mu s}{2\pi}\int_{b-a}^{b+a}\frac{\hat{T}(r',0,s)}{x_1-\xi_1}\hat{\alpha}(\xi_1,h,s)d\xi_1.\end{aligned} \tag{26}$$

Eq. (26) is an integral equation of $\hat{\alpha}$ for a given $\hat{\sigma}_0$. It may be shown that as $\xi_1 \to x_1$, $\hat{T}(0,0,s) \to 1$. Thus Eq. (26) is a singular integral equation of Cauchy's type.

Consider next M non-collinear parallel cracks located at $|x_1 - b_j| \leqslant a_j$ and $x_2 = h_j$, $j = 1,\ldots,M$. Eq. (25) can be generalized for the multiple crack problems as

$$\begin{aligned}\hat{\sigma}_0(x_1,x_2,s) = &-\frac{\mu s}{2c}\sum_{j=1}^{M}e^{\frac{-|x_2-h_j|}{c}s}\int_{x_1}^{b_j+a_j}\hat{\alpha}(\xi_1,h_j,s)d\xi_1 H(a_j-|x_1-b_j|)\\ &+\frac{\mu s}{2\pi}\sum_{j=1}^{M}\int_{b_j-a_j}^{b_j+a_j}\frac{\cos\theta_j'}{r_j'}\hat{T}(r_j',\theta_j',s)\hat{\alpha}(\xi_1,h_j,s)d\xi_1 + \hat{\sigma}_0(x_1,x_2,s),\end{aligned} \tag{27}$$

where $r_j' = \sqrt{(x_1-\xi_1)^2 + (x_2-h_j)^2}$, $\theta_j' = \tan^{-1}\frac{x_2-h_j}{x_1-\xi_1}$. The traction-free conditions at the crack lines then lead to

$$\begin{aligned}\hat{\sigma}_0(x_1,h_i,s) = &\frac{\mu s}{2c}\sum_{j=1}^{M}e^{\frac{-|x_2-h_j|}{c}s}\int_{x_1}^{b_j+a_j}\hat{\alpha}(\xi_1,h_j,s)d\xi_1 H(a_j-|x_1-b_j|)\\ &-\frac{\mu s}{2\pi}\sum_{j=1}^{M}\int_{b_j-a_j}^{b_j+a_{ji}}\frac{\cos\theta_j'}{r_j'}\hat{T}(r_j',\theta_j',s)\hat{\alpha}(\xi_1,h_j,s)d\xi_1,\end{aligned} \tag{28}$$

for $i = 1,2\ldots,M$. Let $x_1 = b_i + a_i x$, $\xi_1 = b_j + a_j\xi$. Moreover, to incorporate the square-root singularity of $\hat{\alpha}$ at $\xi_1 = b_j \pm a_j$, let

$$\hat{\alpha}(b_j + a_j\xi, h_j, s) = \frac{\hat{g}_j(\xi,s)}{a_j\sqrt{1-\xi^2}}, \tag{29}$$

where $\hat{g}_j(\xi,s)$ is finite at $\xi = \pm 1$. Eq. (28) may be rewritten as

$$\begin{aligned}\hat{\sigma}_0(b_i+a_i x,h_i,s) = &\frac{\mu s}{2c}\sum_{j=1}^{M}e^{\frac{-|x_2-h_j|}{c}s}\int_{(b_i-b_j+a_i x)/a_j}^{1}\frac{\hat{g}_j(\xi,s)}{\sqrt{1-\xi^2}}d\xi H(a_j-|a_i x+b_i-b_j|)\\ &-\frac{\mu s}{2\pi}\sum_{j=1}^{M}\int_{-1}^{1}\frac{\cos\theta_j'}{r_j'}\hat{T}(r_j',\theta_j',s)\frac{\hat{g}_j(\xi,s)}{\sqrt{1-\xi^2}}d\xi.\end{aligned} \tag{30}$$

Eq. (30) can be expressed in terms of Gauss–Chebyshev quadrature as (Wu et al., 2013)

$$\begin{aligned}\hat{\tau}_i^{(\ell)} = &\frac{\mu s}{cN}\sum_{j=1}^{M}e^{\frac{-|h_i-h_j|s}{c}}\sum_{k=1}^{N}\left[\left(\sum_{m=1}^{N-1}\frac{\cos(m\phi^{(k)})\sin(m\chi_{ij}^{(\ell)})}{m}\right)\right]\hat{g}_j^{(k)}\\ &-\frac{\mu s}{2N}\sum_{j=1}^{M}\sum_{k=1}^{N}\frac{\cos\theta_{ij}^{\ell k}}{r_{ij}^{\ell k}}\hat{T}(r_{ij}^{\ell k},\theta_{ij}^{\ell k},s)\hat{g}_j^{(k)},\end{aligned} \tag{31}$$

where

$$\begin{aligned}&\hat{\tau}_i^{(\ell)} = \hat{\sigma}_0(b_i + a_i x^{(\ell)}, h_i, s), \quad \hat{g}_j^{(k)} = \hat{g}_j(\xi^{(k)},s)\\ &\xi^{(k)} = \cos(\phi^{(k)}), \quad \phi^{(k)} = (k-1/2)\pi/N, \quad k = 1,2,\ldots,N\\ &x^{(\ell)} = \cos(\psi^{(\ell)}), \quad \psi^{(\ell)} = \ell\pi/N, \quad \ell = 1,2,\ldots,N-1\\ &\chi_{ij}^{(\ell)} = \cos^{-1}\left(\frac{a_i x^{(\ell)} + b_i - b_j}{a_j}\right)H(a_j - |a_i x + b_i - b_j|)\\ &r_{ij}^{\ell k} = \sqrt{(b_i + a_i x^{(\ell)} - b_j - a_j\xi^{(k)})^2 + (h_i - h_j)^2}\\ &\theta_{ij}^{\ell k} = \tan^{-1}\left(\frac{h_i - h_j}{b_i + a_i x^{(\ell)} - b_j - a_j\xi^{(k)}}\right)\end{aligned} \tag{32}$$

and the following crack closure conditions from Eq. (22) have been utilized:

$$\sum_{k=1}^{N}\hat{g}_j^{(k)}=0,\quad j=1,\ldots,M. \tag{33}$$

Eqs. (31) and (33) can be used to determine $\hat{g}_j^{(k)}$, $j=1,\ldots,M$ and $k=1,\ldots,N$.

The stress intensity factors (SIFs) of the crack tips $x_1=b_i\pm a_i$ and $x_2=h_i$ in the Laplace transform domain can then be obtained by (Wu and Chen, 2011)

$$\hat{K}_{\mathrm{III}}(b_i+a_i,h_i,s)=\frac{\mu}{2N}\sqrt{\frac{\pi}{a_i}}\sum_{k=1}^{N}(-1)^{k+1}\cot\frac{\phi^{(k)}}{2}\hat{g}_i^{(k)},$$
$$\hat{K}_{\mathrm{III}}(b_i-a_i,h_i,s)=(-1)^N\frac{\mu}{2N}\sqrt{\frac{\pi}{a_i}}\sum_{k=1}^{N}(-1)^{k+1}\tan\frac{\phi^{(k)}}{2}\hat{g}_i^{(k)}. \tag{34}$$

The inversion of Eq. (34) to the time domain may be carried out using the numerical method proposed by Miller and Guy (1966). The numerical method requires evaluations of Eq. (34) at $s=(\beta+1+k)\delta$, $k=0,1,2,\ldots,N_s$.

5. Numerical examples

Eqs. (31) and (33) were first applied to calculate the SIF for a crack of length $2a$ under the normal incidence of a step plane SH stress wave, $\sigma_{32}(x_1,t)=-\tau_0H(x_2+ct)$, in which case an exact solution (Ing and Ma, 1997) is available for comparison. The cases of two or three parallel cracks of length $2a$ under the same SH stress wave were then considered. In all numerical examples Eqs. (31) and (33) were solved with $N=21$ and the inversion of Eq. (34) was performed based on $\beta=-0.5$, $\delta=0.15$, and $N_s=18$. Variations of the SIFs normalized by $\tau_0\sqrt{\pi a}$ were calculated for $0<ct/a<20$.

5.1. One crack

Consider a crack on the x_1 axis with the center located at the origin. Variation of the SIF as a function of time is shown in Fig. 2. For comparison purposes, the exact solution (Ing and Ma, 1997) is also shown for $0<ct/a<6$. The SIF starts to increase at $t=0$, when the tips are loaded by the stress wave. The SIF continues to increase and reaches a maximum value at $ct/a=2$, when the diffracted wave from one tip arrives at the other tip. The SIF then oscillates near the static value due to the diffracted waves traveling between the tips and is almost indistinguishable from the static value for $ct/a>8$. The numerical result is in a close agreement with the exact solution.

5.2. Two parallel cracks

Consider two cracks parallel to the x_1 axis as shown in Fig. 3. The center of crack A_1B_1 coincides with the origin. The center of crack A_2B_2 is located at $x_1=b$ and $x_2=-0.5a$. Calculations were carried out for $b=0$, a, $3a$, which represent three different degrees of overlap. The two cracks overlap completely or partially when $b=0$ or $b=a$, respectively. For $b=3a$, the cracks do not overlap. Regardless of the value of b, crack A_1B_1 is struck by the SH wave first at $t=0$, when the SIFs associated with tips A_1 and B_1 begin to increase. The stress wave is then reflected by A_1B_1 and diffracted by tip A_1 as well as tip B_1. Tips A_2 and B_2 are loaded only when the diffracted wave or the incident SH wave arrives.

Variations of the SIFs associated with each crack tip for $b=0$ are shown in Fig. 4. For comparison the corresponding static value, which is 0.8, is also plotted in Fig. 4. The diffracted wave and the incident wave arrive at tips A_2 and B_2 at $ct/a=0.5$. The peak normalized SIF of tip A_1 or B_1 is 1.127 at $ct/a=1.9$ and is 1.138 of tip A_2 or B_2 at $ct/a=3.5$. This dynamic overshoots are about 41% above the static value. This is higher than 27% for the case of one crack. Subsequent reflections between the cracks lead to decaying oscillations of the SIFs about the static value. The static value is approached as $ct/a>20$, which is

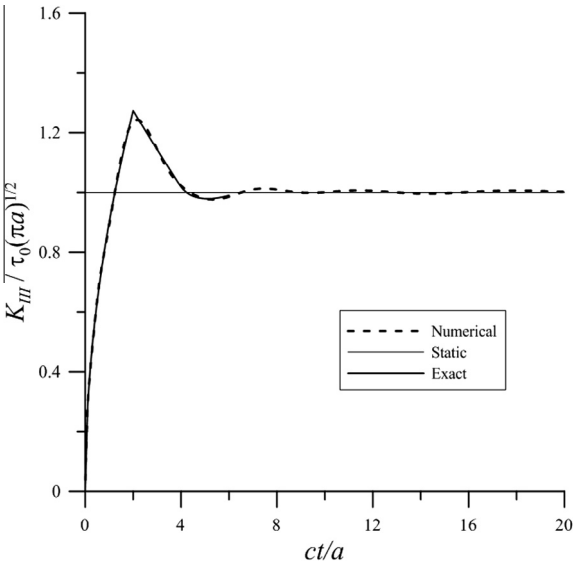

Fig. 2. Variation of the SIF for a crack of length $2a$ subjected to a step plane SH stress wave of τ_0.

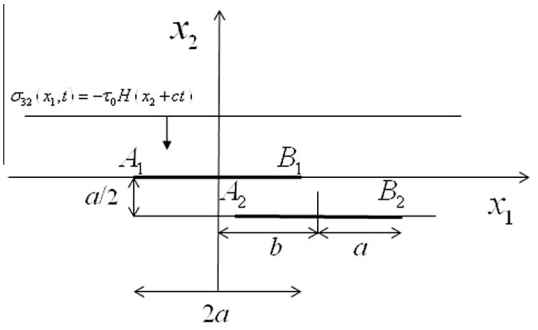

Fig. 3. Configuration of two parallel cracks of length $2a$ subjected to a step plane SH stress wave of τ_0 in an infinite body with shear wave speed c.

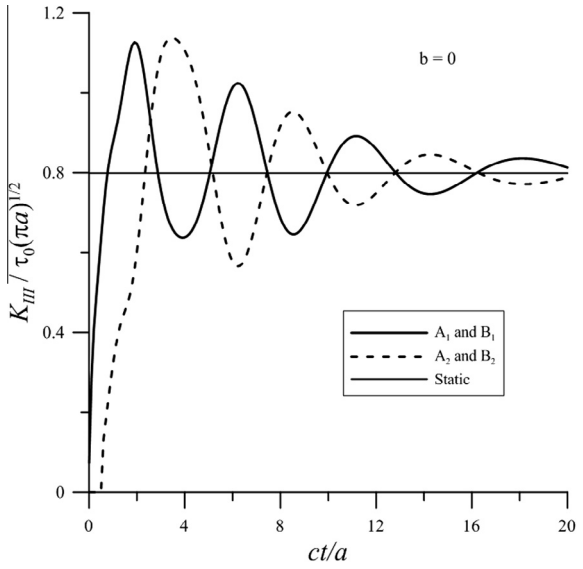

Fig. 4. Variations of the SIFs for two parallel cracks subjected to a step plane SH stress wave with $b = 0$.

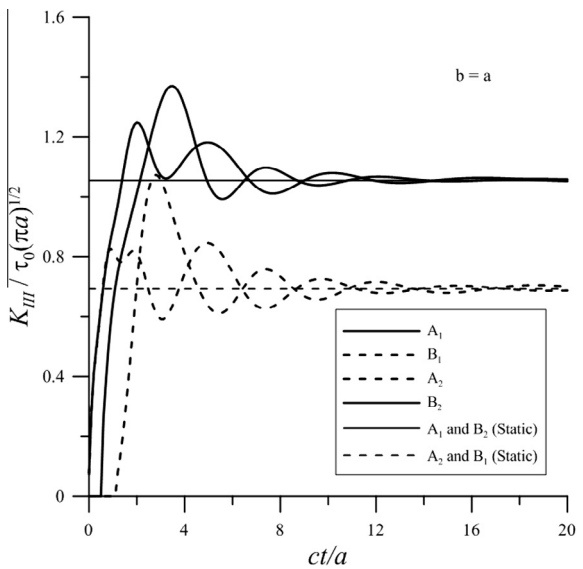

Fig. 5. Variations of the SIFs for two parallel cracks subjected to a step plane SH stress wave with $b = a$.

considerably longer than that for one crack. Our results agree well with those reported by Takakuda et al. (1984), who gave the results only for $ct/a < 6$.

Variations of the SIFs for $b = a$ are given in Fig. 5. The corresponding static values are 1.054 for tip A_1 or B_2 and 0.692 for tip A_2 or B_1. Tip B_2 is not loaded until the stress wave arrives at $ct/a = 0.5$. However, because the stress wave is reflected by crack A_1B_1, the first waves reaching tip A_2 are those diffracted by tips A_1 and B_1. The arrival time is $ct/a = 1.12$. The peak normalized SIF of tip A_1 is 1.249 at $ct/a = 2.0$, 1.073 of tip A_2 at $ct/a = 2.8$, and 1.370 of tip B_2 at $ct/a = 3.5$. This maximum dynamic

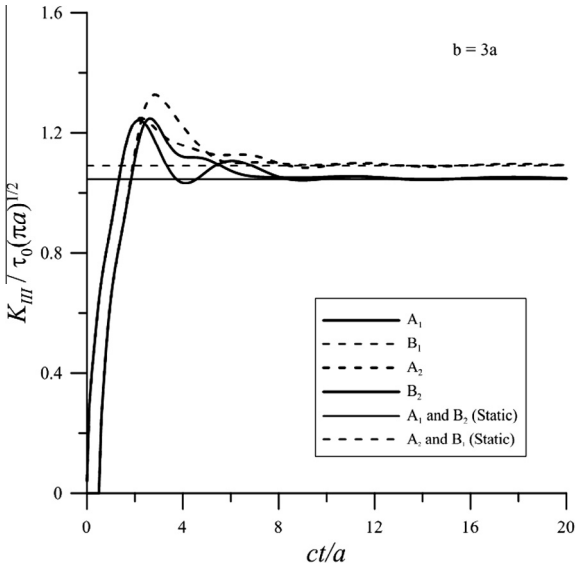

Fig. 6. Variations of the SIFs for two parallel cracks subjected to a step plane SH stress wave with $b = 3a$.

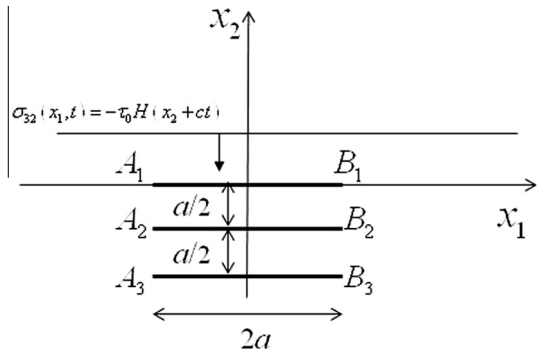

Fig. 7. Configuration of three parallel cracks of length $2a$ subjected to a step plane SH stress wave.

overshoot is about 55% at tip A_2. The static values are reached as $ct/a > 14$, which is sooner than that for $b = 0$.

Variations of the SIFs for $b = 3a$ are displayed in Fig. 6. The corresponding static values are 1.046 for tip A_1 or B_2 and 1.090 for tip A_2 or B_1. Either tip A_2 or tip B_2 is loaded by the stress wave as $ct/a > 0.5$. The peak normalized SIF of tip A_1, B_1, or B_2 are essentially the same as that for one crack. However, the peak normalized SIF of tip A_2 is increased to 1.327 at $ct/a = 2.8$. The maximum dynamic overshoot is about 22% at tip A_2. The static values are reached as soon as $ct/a > 8$ similar to the case of one crack.

5.3. Three parallel cracks

Consider three cracks parallel to the x_1 axis as shown in Fig. 7. The centers of the cracks A_1B_1, A_2B_2 and A_3B_3, respectively, are located at $(0, 0)$, $(0, -0.5a)$ and $(0, -a)$. Variations of the SIFs are shown in Fig. 8. The SH wave arrives tip A_1 or B_1 at $t = 0$. The diffracted wave and the incident wave arrive at tip A_2 or B_2 at $ct/a = 0.5$ and tip A_3 or B_3

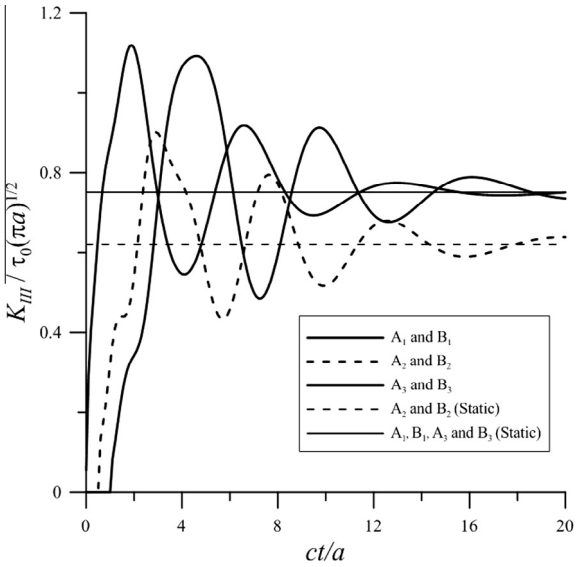

Fig. 8. Variations of the SIFs for three parallel cracks subjected to a step plane SH stress wave.

at $ct/a = 1$. The corresponding static value is 0.751 for tip A_1 (B_1) or A_3 (B_3) and 0.620 for tip A_2 (B_2). The peak normalized SIFs of tip A_1 (B_1), A_2 (B_2), and A_3 (B_3), respectively, are 1.120 at $ct/a = 1.9$, 0.902 at $ct/a = 2.9$, and 1.093 at $ct/a = 4.6$. The dynamic overshoots are over 45%. Similar to the previous case of two cracks with $b = 0$, multiple reflections between the cracks occur and the static values are reached for $ct/a > 20$.

6. Conclusions

A space–time integral equation for multiple parallel cracks under dynamic anti-plane shear loading has been derived. The formulation was based on the fundamental dynamic solution of a screw dislocation. The integral equation in the Laplace transform domain was solved by Gaussian–Chebyshev integration quadrature, which is commonly employed for static crack problems. The dynamic stress intensity factor associated with each crack tip was calculated by a numerical inverse Laplace scheme. The numerical examples show that higher dynamic overshoots than that for a single crack might be induced and that it took longer time to approach to the steady state if multiple reflections between the cracks occurred.

Acknowledgment

The research was supported by the National Science Council of Taiwan under Grant NSC 101-2221-E-002-086-MY2.

References

Ayatollahi, M., Monfared, M.M., 2012. Anti-plane transient analysis of planes with multiple cracks. Mech. Mater. 50, 36–46.
Chen, W., Tang, R., 1996. Cauchy singular integral equation method for transient antiplane dynamic problems. Eng. Fract. Mech. 54, 177–187.
Cochard, A., Madariaga, R., 1994. Dynamic faulting under rate-dependent friction. Pure Appl. Geophys. 142, 419–445.
Erdogan, F., Gupta, G.D., Cook, T.S., 1973. Numerical solution of singular integral equations. In: Sih, G.C. (Ed.), Methods of Analysis and Solutions of Crack Problems. Noordhoff, Leyden, pp. 368–425.
Ing, Y.S., Ma, C.C., 1997. Dynamic fracture analysis of a finite crack subjected to an incident horizontally polarized shear wave. Int. J. Solids Struct. 34, 895–910.
Miller, M.K., Guy Jr, T., 1966. Numerical inversion of the Laplace transform by use of Jacobi polynomials. SIAM J. Numer. Anal. 3, 624–635.
Morrissey, J.W., Geubelle, P.H., 1997. A numerical scheme for mode III dynamic fracture problems. Int. J. Numer. Methods Eng. 40, 1181–1196.
Takakuda, K., Takizawa, Y., Koizumi, T., Shibuya, T., 1984. Dynamic interactions between cracks: diffractions of SH waves which are incident on Griffith cracks in an infinite body. Bull. JSME 27, 2605–2610.
Wu, K.-C., Chen, J.-C., 2011. Transient analysis of collinear cracks under anti-plane dynamic loading. Proc. Eng. 10, 924–929.
Wu, K.-C., Huang, S.-M., Chen, S.-H., 2013. Dynamic stress intensity factors of collinear cracks under a uniform tensile stress wave. CMES. Comput. Model. Eng. Sci. 93, 133–148.
Wu, K.C., 1999. Dynamic green's functions for anisotropic materials under anti-plane deformation. J. Mech. 15, 11–16.